DEUTSCHES ELEKTRONEN-SYNCHROTRON DESY

DESY SR-81/06
September 1981

Kr AND Xe GUEST ATOMS IN Ar MATRIX: EMISSION SPECTRA, EXCITATION SPECTRA AND LIFETIMES

by

U. Hahn, R. Haensel and N. Schwentner
Institut für Experimentalphysik der Universität Kiel

NOTKESTRASSE 85 · 2 HAMBURG 52

To be sure that your preprints are promptly included in the
HIGH ENERGY PHYSICS INDEX ,
send them to the following address (if possible by air mail) :

DESY
Bibliothek
Notkestrasse 85
2 Hamburg 52
Germany

DESY SR-81/06
September 1981

Kr and Xe Guest Atoms in Ar Matrix: Emission Spectra, Excitation Spectra and Lifetimes

U. Hahn[+], R. Haensel and N. Schwentner
Inst. für Exp. Physik, Univ. Kiel, 2300 Kiel, FRG

Subject classification: 13.4, 20.3, 23

Abstract

Emission bands of isolated Kr and Xe atoms in solid Ar matrices are assigned to atomic $^3P_1$ and $^1P_1$ states on the basis of excitation and emission spectra. The temperature and concentration dependence of these spectra is used to sort out emission from distorted sites. The dependence of the liftetimes on temperature reflects the competition between radiative and nonradiative decay.

Emissionsbanden von Kr und Xe Atomen, die in festen Ar Matrizen isoliert sind, werden den atomaren $^3P_1$ und $^1P_1$ Zuständen auf Grund von Anregungs- und Emissionsspektren zugeordnet. Die Emissionsbanden von gestörten Zentren lassen sich an Hand des Einflusses der Konzentration und der Temperaturbedingungen auf diese Spektren abtrennen. Die Abhängigkeit der Lebensdauern von der Temperatur spiegelt die Konkurrenz von strahlenden und strahlungslosen Zerfällen wieder.

[+] Now at Deutsches Elektronen-Synchrotron, Hamburg, HASYLAB.

1. Introduction

Rare gas matrices doped with rare gas atoms served as examples to discuss various problems including the nature of electronic states of guest atoms (1-7), the pathways and efficiencies of energy transfer processes from the matrix to guest atoms (7-10), the relaxation in the manifold of guest atomic states (5, 6, 9, 11), the formation of bubbles around excited guest atoms (5, 11, 12, 13) of homonuclear guest molecules (11, 12, 13, 14) and of heteronuclear guest-matrix molecules (11, 12). The primary excited states are known from absorption (1,2, 13) and photoelectron spectroscopy (3, 9). The relaxation cascade connecting the primarily excited states with the emitting states has been studied recently in detail for Xe, Kr and Ar guest atoms in a Ne matrix by time resolved excitation and emission spectroscopy (5). For Xe and Kr guest atoms in Ar matrix the luminescence bands have been observed after ionizing excitation with electrons (12), X-rays (15) and α particles (11). Some experiments with optical excitation have been performed for Xe in Ar (14, 16, 17). The emission bands have been assigned in analogy to gas phase data to atomic impurity states and to homonuclear and heteronuclear molecular impurity states. We present excitation spectra for the emission bands of Kr and Xe atoms in Ar matrix to identify the emission from isolated guest atoms which are placed at undistortet lattice sites. Emission bands which can be excited by photon energies below the threshold for absorption of isolated atoms and which are sensitive on annealing and on concentration are attributed to guest atoms at distorted lattice sites. In this way, we try to sort out emission from guest atoms at sites which are connected to voids, to next nearest neighbors, to nearest neighbors or to clusters of guest atoms. Decay curves support the assignment of emission bands. The temperature dependence of the decay curves provides information about the balance of radiative and radiationless processes. The investigations of Refs. 16 and 17 are extended to excitation energies below the onset of the matrix absorption. Compared to Ref. 14, we are able to separate the individual emission bands in the measurement of excitation spectra completely.

2. Experimental Conditions

For excitation purposes the synchrotron radiation of the storage ring DORIS in Hamburg has been monochromatized with a bandpass of $\sim$ 2 Å. The dispersed light has been focused onto the sample which has been cooled by a liquid He flow cryostat to temperatures between 300 K and 5 K. The emitted light has been dispersed with a band width of $\sim$ 20 Å and has been detected by a microchannel plate. The emission spectra are not corrected for the wavelength dependence of the efficiency of the detector. The efficiency decreases monotonically by a factor of 4 in going from 10 eV to 8 eV. The excitation spectra are corrected for the wavelength dependence of the intensity of the incoming light. For the decay time measurements the short pulse width of the light flash of 130 psec, the high repetition rate of 125 MHz and the small jitter of the microchannel plate have been exploited in the single photon counting technique. In this way, a total width of the response function of 400 psec has been obtained. By deconvolution decay times down to 50 psec have been determined. The experimental set up (18) and the data handling (5) are described in more details elsewhere.

The gases have been mixed with partial pressures according to the indicated concentration in an ultra high vacuum gas handling system. They have been deposited as thin films with thicknesses between 1 µ and 100 µ on the substrate at a temperature of 6 K and a background pressure of 10^{-9} mbar. The purity of the gases was: Ar (99.9997 %); Kr (99.997 %); Xe (99.997 %). The observed intensities and decay times did not depend on time after preparation within some hours. After annealing of the films at 15 - 20 K for about 15 minutes, the spectra, lifetimes and their temperature dependence have been reproducible for all films. Also changes due to annealing have been reproducible.

3. Emission bands for Kr atoms in Ar matrix

An overview on the emission bands of Kr guest atoms is shown in Fig. 1a for low (0.03%) and high (3%) guest atom concentration. The excitation

energy of 13.8 eV corresponds to the region of the n = 2 to n = 3 excitons of the Ar matrix and the light is absorbed mainly in the bulk of the matrix. By energy transfer processes probably all the different emitting states of Kr atoms are populated. These conditions are similar to excitation with ionizing radiation. In the following arguments will be given for an assignment of the bands a and b to Kr atoms at substitutional undistorted sites in excited states similar to the atomic $^3P_1$ and $^1P_1$ states respectively. Band c corresponds to an excimer-like emission Kr_2^* due to pairs or clusters of Kr guest atoms. The bands d, e and f are attributed to excited states of Kr atoms at distorted lattice sites which can include sites with next nearest neighbours of Kr atoms or Kr atoms in the neighbourhood of voids or perhaps excited heteronuclear molecules Kr^*Ar. Finally, bands g and h are due to the Ar matrix. g corresponds to emission from vibrationally relaxed Ar_2^* excimer centers and h belongs either to vibrationally hot Ar_2^* centers or to atomic like Ar^* centers. The emission bands of Fig. 1 are listed in Table I and compared with earlier experiments using ionizing radiation. The identification of the bands g and h is evident from the similar energies and intensities in pure solid Ar (17), from the decrease in intensity with larger Kr concenteration, i.e. more efficient energy transfer to guest atoms (Fig. 1a) and from the absence of these bands for excitation energies lower than the Ar n = 1 exciton energy (Fig. 1b - 1d).

The origin of the bands a and b follows from a comparison of the excitation spectra of these bands (Fig. 2b and 2c) with absorption spectra of Kr atoms in Ar matrix (Fig. 2a). Due to the limited film thickness, the samples are essentially transparent for photon energies below the n = 1 exciton of the Ar matrix ($\sim$ 12 eV) except at energies corresponding to a high absorption coefficient of the Kr atoms in the matrix. Therefore we expect a close similarity between the excitation and absorption spectra. The first maximum in the excitation spectrum of band a (Fig. 2b) reproduces the absorption band of the n = 1 exciton of the Kr guest atoms in the Ar matrix (Fig. 2a) which corresponds to the $^3P_1$ transition of free Kr atoms. Thus band a is attributed to the Kr $^3P_1$ state. The absorption band is shifted by 0.79 eV to the blue compared to the gas phase and the emission band lies halfway between the matrix absorption and the gas phase value (Tab. 2). In the same way, the emission band b (Fig. 2c) can be identified with the n' = 1 Kr exciton in the matrix (Fig. 2a) and with the $^1P_1$ state of the free atom. The shifts between

absorption, emission and gas phase energies are very similar for both bands a and b (Tab. 2). These shifts are very large compared to the matrix phonon energies of about 5 meV. The large gas to matrix shift in absorption indicates a strong electron phonon coupling between the excited Kr atoms and the surrounding Ar lattice. The large relaxation energy given by the difference between absorption and emission demonstrates an appreciable rearrangement of the matrix atoms around the excited atoms. The energy shift in direction to the gas phase value suggests a bubble like rearrangement (5).

A variation of the concentration and the annealing conditions (Fig. 1b, c) shows that only the bands a and b remain in well annealed samples of low doping concentration. Therefore, these bands are assigned to isolated Kr atoms at undistorted lattice sites. In these sites a substitutional replacement of Ar atoms by Kr atoms is likely, since the internuclear separation in the ground state of a free Ar - Kr molecule of 3.80 Å - 3.94 Å (19) is only slightly larger than the nearest neighbor separation of 3.755 Å in an Ar crystal. The bands a and b accidentally coincide with emission bands of N atoms in Ne matrix (20), but an assignment to N atoms (15) has to be rejected for our samples.

Emission band c coincides in energy with the second continuum of free Kr_2^* excimers and with the main emission band of solid Kr due to Kr_2^* excimer like centers in the crystal. The intensity of band c increases with the concentration (Fig. 1) and an assignment to Kr_2^* centers at pairs or clusters of Kr atoms in the Ar matrix is evident (Table 1).

Emission bands d and e (Fig. 1d, 2d) can be excited with energies below the onset of absorption of isolated Kr atoms in the Ar matrix (Fig. 2a). An excitation spectrum of band d for example (Fig. 2d) shows an onset around 10 eV which is similar to the first absorption of solid Kr and also of free Kr atoms, but which is 1 eV below the n = 1 Kr exciton in Ar matrix (Table 1). Therefore, Kr atoms near voids and/or pairs of next nearest neighbor Kr atoms may be responsible for these emissions. The energy of band e lies near the energy of free Kr atoms. The energy of band d is situated between the energy of free Kr atoms and of Kr_2^* excimers. Perhaps

band e belongs to Kr sites at voids and band d to next nearest neighbor Kr pairs. Band e has also been attributed to heteronuclear molecules Kr^* Ar (11, 12, 15). The strong increase in intensity of band d and e with concentration compared to the bands a and b (Fig. 1b, c) supports an assignment to next nearest neighbor pairs but also to defects like voids which can be caused by the distortions in the matrix due to the dopand. The reduction of band d and e after annealing is a further indication for the contribution of defects to these emissions. An assignment of band d to Kr^* Ar molecules would mean that the formation of these centers is induced by lattice distortions or by the presence of next nearest Kr neighbors. The weak emission band f behaves similar to the bands d and e and it is attributed to an unidentified site (Tab. 1).

A comparison of the intensities in the emission bands with a statistical distribution of the Kr atoms in substitutional places of the fcc lattice is obvious, since electron diffraction studies (21) showed that Kr and Ar mixtures form polycrystalline films without segregation of the components for similar preparation conditions. For a Kr concentration of 3% it is expected that 58% of the Kr atoms are in isolated sites, 19% have a next nearest neighbor Kr atom and 23% are pairs or larger clusters of Kr atoms (22). The emission spectrum for 3% Kr in Fig. 1a yields relative intensities for the bands a to e of 8%, 18%, 18%, 26%, 30% respectively, after a rough correction for the sensitivity of the detection system. This means that band a and b contribute together 26% to the isolated sites and band c about 18% to the Kr pairs. If we assume that band d stems from next nearest neighbor pairs and band e from isolated Kr atoms at voids (see above), then we come to 56% at isolated sites, 26% at sites with next nearest Kr neighbors and 18% of pairs and clusters. This estimate is in surprisingly good agreement with the expected distribution.

4. Lifetimes of Kr $^3P_1$ and $^1P_1$ states in Ar matrix

The rise times for the bands a and b for excitation of n = 1 and n' = 1 Kr excitons are shorter than our detectable limit of 10 psec. Therefore the matrix relaxation which leads to the population of the emitting states is extremely fast ($<10^{-11}$ sec) as in a Ne matrix (5). The decay times at 6 K (Table 3) are shorter by a factor of about 4 than corresponding radiative

lifetimes in the gas phase and in the Ne matrix (5). Local field corrections and the blue shift can explain only a shortening up to a factor of 1.5 (5). The strong influence of radiationless processes on the lifetime of the $^3P_1$ state of Kr in Ar (band a) follows from the strong reduction of the intensity and of the lifetime of this transition with increasing temperature.

From 6 K to 28 K the lifetimes go down from 850 ps to 60 ps (Fig. 3a). The proportional decrease of the intensity indicates radiationless quenching of the $^3P_1$ population. The rate constants W(T) shown as crosses in Fig. 3a have been described by a sum of rate constants for radiative decay, W_s and nonradiative relaxation $W_{ns}(T)$.

$$W(T) = W_s + W_{ns}(T).$$

For W_s the value of $W_s = 5 \times 10^8\ s^{-1}$ for Kr in Ne has been used. W_{ns} has been fitted by an expression derived by Jortner (23) within a configuration coordinate model for energy transfer and radiationless electronic relaxation.

$$W_{ns} = A \exp\{-S(2v+1)\} \cdot \{(v+1)/v\}^{N/2} \cdot I_N\{2S\{v(v+1)\}^{1/2}\}$$

$$A = 2\pi |V_{ab}|^2/\hbar^2/\omega_p$$

$$v = \{\exp(\hbar\omega_p/kT) - 1\}^{-1}$$

$$N = \Delta E/\hbar\omega_p$$

S is the electron-phonon coupling strength, $I_N\{z\}$ a modified Bessel function, V_{ab} the electronic matrix element, $\hbar\omega_p$ a mean phonon frequency of the system. ΔE corresponds to the energy gap between the minima of initial and final nuclear potential surfaces and N is the number of phonons emitted in the relaxation process. A fit of the shape of the experimental temperature dependence of W(T) leads to 4 meV $\leq \hbar\omega_p \leq$ 6 meV and restricts S and N to the area between the dashed lines in Fig. 3b. An upper limit for V_{ab} of $|V_{ab}| \leq 1$ eV together with the experimental value of the transition rate at 20 K requires values of S which are larger than the border indicated by the solid line in Fig. 3b. This border restricts S and N to the dashed area in Fig. 3b.

A further specification of the parameters S, N, V_{ab}, $\hbar\omega_p$ requires a choice of the electronic states involved. Plausible relaxation processes are nonradiative relaxation to the ground state or to the $^3P_2$ state which are the only lower lying states in the Kr atom or energy transfer to centers emitting band c, d, e or to an unidentified species. Relaxation to the ground state is unimportant, because N would be of the order of 2000 requiring a coupling constant S > 1000 (Fig. 3b), whereas the fwhm of the transition in absorption of 110 meV (1) limits S to S < 150. Energy transfer to the centers responsible for the bands c, d, e can be excluded, because the intensity missing in band a at higher temperatures does not appear in those bands. Also additional emission bands from unidentified centers have not been observed. The $^3P_1$ state is probably depopulated by nonradiative relaxation to the $^3P_2$ state which lies in the gas phase 82 meV below the $^3P_1$ state. The energy gap ΔE is given by the splitting of the $^3P_1$ and $^3P_2$ state in the matrix which can be slightly changed in the matrix due to a different gradient of the potential. The electronic matrix element V_{ab} is due to the spin-orbit interaction of the excited Kr electron in this case which causes also the splitting of $^3P_1$ and $^3P_2$. Therefore, the value of $|V_{ab}|$ should be of the same order of magnitude as the splitting. The dashed area in Fig. 3b allows a choice of parameters which is consistent with this explanation. A possible choice is N = 30, S = 9, $\hbar\omega_p$ = 4 meV which yields ΔE = 120 meV and $|V_{ab}|$ = 135 meV. Fits for the temperature dependence of the transition rate for similar parameters are shown in Fig. 3a. The range of consistent parameters extends to N = 50, S = 21, $\hbar\omega_p$ = 4 meV yielding ΔE = 200 meV and $|V_{ab}|$ = 110 meV.

Radiative decay from the $^3P_2$ state to the ground state is dipole forbidden and the intensity stored in the $^3P_2$ state has to be quenched nonradiatively to the ground state or to a state emitting below the detector threshold at 7 eV as follows from the decrease in the intensity. This is different to the case of Kr in Ne matrix where no relaxation from $^3P_1$ to $^3P_2$ has been observed and where, when populated, the $^3P_2$ state decays radiatively, but with a long lifetime (5).

The lifetime and the intensity of the $^1P_1$ state of Kr in Ar does not depend on temperature up to 28 K. This is surprising, because of the presence of the $^3P_0$ state which lies in the free atom also only 82 meV below the $^1P_1$ state. Further, the intensity of band a ($^3P_1$) is practically zero for

excitation of the n' = 1 ($^1P_1$) exciton (Fig. 2b) in well annealed samples with low concentration (0.03%). This indicates that no intraatomic nonradiative relaxation from $^1P_1$ to $^3P_1$ takes place. According to the statistics in the experiment a lower limit of 65 nsec for this relaxation time is derived. With increasing Kr concentration the $^3P_1$ emission can be excited through the n' = 1 exciton reaching the same probability like by direct n = 1 excitation at 3%. Reabsorption could explain this observation, because the $^1P_1$ emission (band b) nearly coincides with the n = 1 absorption band of Kr. More probable is resonant interatomic energy transfer between an excited Kr atom in the $^1P_1$ state and a nearby Kr atom in the ground state. This energy transfer has been observed also for Kr in Ne (5) with a Förster Dexter radius of about 21 Å.

Finally at high Kr concentrations the lifetimes of the $^3P_1$ and $^1P_1$ states are shortened (Table 3). The dominant process will be resonant energy transfer to the centers which emit the bands d and e, since the spectral overlap with the absorption spectrum of the "site centers" is large according to the excitation spectrum in Fig. 2d. The corresponding excitation energies indeed lead to the emission bands d and e (Fig. 1d).

The decay curves of the bands d and e contain a long living backbround (Table 3) which is characteristic for molecular centers in rare gases (10, 24) and which is observed also for the homonuclear molecular emission c. The short components in the decay curves of the bands c, d and e are rather similar (Table 3).

5. Excitation and Emission Spectra for Xe in Ar

Fig. 4 shows the set of four emission bands "a, b, c, d" (Table 4) which we observed for different excitation energies. From a comparison of the excitation spectra (Fig. 5b-d) with the absorption spectrum (Fig. 5a) it follows immediately that band b corresponds to the n = 1 (i.e. $^3P_1$) exciton state and band a to the n = 2 exciton state of isolated Xe atoms in an Ar matrix. The up to now (Table 4) mainly considered bands c and d are excited preferentially far below the n = 1 exciton of Xe atoms in Ar matrix, also in the transparent region between n = 1 and n = 2 excitons and in the weak absorbing region of higher Xe exciton bands in Ar (Fig. 5d, only for band d). The onset (Fig. 5d) in the excitation spectra of

emission c and d is similar to the threshold of absorption of free Xe atoms or of pure solid Xe suggesting an assignment to emission from special sites either connected to clusters or voids. The appearance even at low Xe concentration (0,01%) favours the asignment to voids.

The $^3P_1$ (n=1) state can only be populated by direct excitation of the n = 1 exciton (Fig. 5c). No radiative or nonradiative relaxation from higher excited states like n = 2, $^3P_0$, $^1P_1$ .... to the $^3P_1$ state takes place which is similar to Xe in Ne (5). The probability for radiationless transitions decreases exponentially with an increasing energy gap between the states involved (5, 6, 23). The gap between the relaxed n = 2 and $^3P_1$ states exceeds 0.9 eV. A crossing of this gap would require an order N of more than 100 for the radiationless transition i.e. an emission of more than 100 matrix phonons in one step. For the lifetime of the $^3P_1$ state we obtained 1.5 nsec. It is about half of the radiative lifetime in the gas phase (25) or in the Ne matrix (5) and seems to be influenced by radiationless processes. The decay time of the emission band a (n = 2) was longer than the pulse separation of 8 nsec given by the repetition frequency of 125 MHz. Such long lifetimes are expected from the n^{-3} law for the oscillator strength in exciton series.

The red shift of the emission bands relative to the absorption bands (Table 4) can be rationalized in a configuration coordinate scheme with the nearest neighbour separation as configuration coordinate. The red shift follows from a bubble like increase of the configuration coordinate (5). The change of the transition energies with bubble radius, i.e. with the mean density of matrix atoms around the excited guest atoms can be estimated from the experimental dependence of the transition energies on the Ar density (5) in absorption spectra of Xe atoms in liquid Ar (26). The emission energies of the $^3P_1$ band corresponds to a reduction of the solid state density of 1.76 g cm^{-3} (26.5 atoms $Å^{-3} \times 10^{-3}$) to about 1.4 g cm^{-3}. For the n = 2 emission band the absorption experiment (26) suggests a crossing of the energy versus density curves of the n = 2 and the $^1P_1$ state. The Ar density in the relaxed configuration is reduced to 1.25 g cm^{-3} and the transition has to be assigned either to the $^1P_1$ or the n = 2 exciton state of the Xe guest atoms. The decrease in density around the $^3P_1$ and $^1P_1$ (n=2) states corresponds to an increase of the bubble radius by about 10% compared to the equilibrium separation in the ground state due to the rearrangement of the matrix.

Xe in Ar has been investigated by α particle (11), X-ray (14, 15), electron (12) and photon excitation (14, 16, 17) (see Table 4). In these experiments the guest atoms have been excited indirectly via energy transfer from the Ar matrix, with the exception of Ref. 14. The use of energy selective converters instead of a secondary monochromator in Ref. 14 allows only to separate the Xe_2^* band from higher energetic emissions. Therefore, the excitation spectra for the high energetic emissions (14) represent a superposition of all contributions and the information about the strong selectivity of the excitation channels for the different emission branches is lost. The strong contribution of the bands c and d to the emission spectra after ionizing excitation and the disappearance of band b can be explained by our excitation spectra. The bands c and d are activated by ionizing excitation due to their high excitation probability (Fig. 5d) at the energy of the Ar_2^* emission band (9.7 eV) which results in an efficient Förster Dexter type energy transfer to these centers. The overlap of the single excitation band of b with the matrix emission is small which prevents an efficient population of the n = 1 and $^3P_1$ state by ionizing excitation.

It is a pleasure to thank the staff of HASYLAB for cooperation, B. Jordan for support in the experiment and G. Zimmerer for discussions. This work has been supported by the Bundesministerium für Forschung und Technologie BMFT.

References

1) G. Baldini, Phys. Rev. 137, 508 (1965)

2) D. Pudewill, F.-J. Himpsel, V. Saile, N. Schwentner, M. Skibowski and E.E. Koch, phys. stat.sol. (b) 74, 485 (1976)

3) R. Kürnberger, F.-J. Himpsel, E.E. Koch and N. Schwentner, phys. stat.sol. (b) 81, 503 (1977)

4) L. Resca, R. Resta, Phys. Rev. B 19, 1683 (1979)

5) U. Hahn and N. Schwentner, Chem. Phys. 48, 53 (1980)

6) J. Jortner in "Vacuum Ultraviolet Radiation Physics" ed. E.E. Koch, R. Haensel and C. Kunz, Pergamon-Vieweg, Braunschweig (1974)

7) N. Schwentner, Appl. Optics 19, 4104 (1980)

N. Schwentner, E.E. Koch and J. Jortner, to appear in "Rare Gas Solids III", ed. M.L. Klein and J.A. Venables, Academic Press (1981)

8) Z. Ophir, B. Raz, J. Jortner, V. Saile, N. Schwentner, E.E. Koch, M. Skibowski and W. Steinmann, J. Chem. Phys. 62, 650 (1975)

9) N. Schwentner, E.E. Koch, Phys. Rev. B 14, 4687 (1976)

10) G. Zimmerer and N. Schwentner in "Luminescence of Inorganic Solids", ed. B. Di Bartolo, Plenum Press, New York (1978), p. 627 and p. 645

11) A. Gedanken, B. Raz and J. Jortner, J. Chem. Phys. 59, 5471 (1973)

12) I. Ya Fugol', Advances in Phys. 27, 1 (1978)

13) T. Nanba, N. Miura, N. Nagasawa, J. Phys. Soc. Jap. 36, 158 (1974)

14) T. Nanba, N. Nagasawa and M. Ueta, J. Phys. Soc. Jap. 37, 1031 (1974)

15) R. Heumüller, Thesis, University of Regensburg 1978

16) H. Möller, Diploma Work, University of Hamburg 1976

17) Ch. Ackermann, Thesis, University of Hamburg 1976

18) U. Hahn, N. Schwentner and G. Zimmerer, Nucl. Instr. and Methods 152, 261 (1978)

19) J.M. Parson, T.P. Schafer, F.P. Tully, Y.C. Wong and Y.T. Lee, J. Chem. Phys. 53, 3755 (1970)

W. Hogevorst, Physica 51, 59 (1971)

J.K. Lee, D. Henderson and J.A. Barker, Mol. Phys. 29, 429 (1975)

20) E. Schuberth and M. Creuzburg, phys. stat. sol. (b) 90, 189 (1978)

W. Böhmer, R. Haensel, N. Schwentner and E. Boursey, Chem. Phys. 49, 225 (1980)

21) A.E. Curzon and A.J. Mascall, J. Phys. C. (Solid State Phys.)2, 220 (1969)

22) M.M. Kreitmann, D.L. Barnett, J. Chem. Phys. 43, 364 (1965)

23) J. Jortner, J. Chem. Phys. 64, 4860 (1976)

24) G. Zimmerer, J. Luminescence 18/19, 875 (1979)

25) E. Matthias, R.A. Rosenberg, E.D. Poliakoff, M.C. White, S.-T. Lee and D.A. Shirley, Chem. Phys. Letters 56, 239 (1977)

26) I. Messing, B. Raz and J. Jortner, Chem. Phys. 23, 23 (1977)

Figure Captions

Fig. 1a - d): Emission spectra for Kr in Ar at 6 K for excitation energies of 13.8 eV, 11.37 eV (n' = 1), 10.78 eV (n=1), 10.65 eV and 10.16 eV, respectively. The excitation energies are marked by arrows. The energies of the emission band a - h are listed in Table 1.——— 0.03% Kr after annealing; ..... 0.03% Kr, -·—·—·— 0.3% Kr, ----- 3% Kr all before annealing.

Fig. 2a): Absorption spectrum for 0.1% Kr in Ar after Ref. 1.

Fig. 2b - d): Excitation spectra for emission bands a($^3P_1$), b($^1P_1$) and d(site) of Fig. 1, respectively at 6 K. The emission energies are marked by arrows. ——0.03% Kr and —·—·—·— 0.3% Kr after annealing; .... 0.03% Kr, -.-.-. 0.3% Kr, ---- 3% Kr before annealing.

Fig. 3a): The experimental temperature dependence of the transition rate of the emission band a ($^3P_1$) for Kr in Ar is shown by crosses. The fits according to the text with N = 30, $\hbar\omega_p$ = 4 meV and values of S = 5 (...), S = 7 (———) and S = 10 (- - - -) have been normalized at 20 K to the experimental value.

Fig. 3b): The dashed area indicates the range of coupling constants S and of orders N of the relaxation process which is consistent with the experimental temperature dependence of the transition rate (see text).

Fig. 4): Emission spectra for 0.01% Xe in Ar at 6 K for excitation energies of 11.07, 9.22, 9.02 and 8.57 eV which are marked by arrows.

Fig. 5a): Absorption spectrum for 0.3% Xe in Ar after Ref. 1.

Fig. 5b - d): Excitation spectra for 0.01% Xe in Ar at 6 K for the emission bands a ($^1P_1$, n = 2), b ($^3P_1$) and d (site) which are marked by arrows.

Table 1: Emission bands for Kr in Ar. The meaning of "sites" is explained in the text. The emission bands are named according to Fig. 1 and the assignments of the authors are included. Energies in eV.

band	this work		α-particles a)		electrons b)		X-rays c)	
c	8.55	Kr_2^*	8.55	Kr_2^*	8.33	Kr_2^*	8.53	Kr_2^*
							8.90	Kr^*Ar
d	9.3	site	9.32	Kr^*Ar	9.26	Kr^*Ar	9.33	Kr^*Ar
g	9.65	Ar_2^*	9.69	Ar_2^*	9.63	Ar_2^*	9.7	Ar_2^*
e	9.9	site						
a	10.4	Kr $^3P_1$	10.33	Kr $^3P_1$			10.42	N
f	10.5	site						
b	10.95	Kr $^1P_1$	10.92	Kr $^3P_1$ site			10.97	N
h	11.5	Ar_2^*,Ar						

a) A. Gedanken, B. Raz, J. Jortner, Chem. Phys. 59, 5471 (1973)

b) Ya Fugol', Advances in Phys. 27, 1 (1978)

c) R.Heumüller, Thesis, Regensburg (1978)

Table 2: Absorption bands (A), emission bands (E) of Kr in Ar matrix and in the free Kr atom (G). Stokes shift between absorption and emission (A-E) and matrix to gas shift of emission (E-G). Energies in eV

	A [a]	E [b]	G	A-E [b]	E-G [b]
$^3P_1$ (n = 1)	10.79	10.4	10.00	0.39	0.40
$^1P_1$ (n' = 1)	11.36	10.95	10.64	0.39	0.31

a) G. Baldini, Phys. Rev. 137, 508 (1965)

b) this work

Table 3: Decay times for the emission bands a, b, c, d, e of Fig. 1 at low and high Kr concentration at 6 K. Relative contribution B of the long background in the decay curve for 3% Kr. Times in 10^{-9} sec.

band		Lifetimes in Ar matrix 0.03 % Kr	3 % Kr	gas phase [a]	B
a	Kr $^3P_1$	0.85 ±0.05	0.4 ±0.05	3.18 ±0.12	
b	Kr $^1P_1$	0.65 ±0.05	0.4 ±0.05	3.11 ±0.12	
c	Kr_2^*		1.5		250
d	site		1.1 ±0.1		40
e	site		1.1 ±0.1		100

a) E. Matthias, R.A. Rosenberg, E.D. Poliakoff, M.C. White, S.-T. Lee and P.A. Shirley, Chem. Phys. Letters 52, 239 (1977)

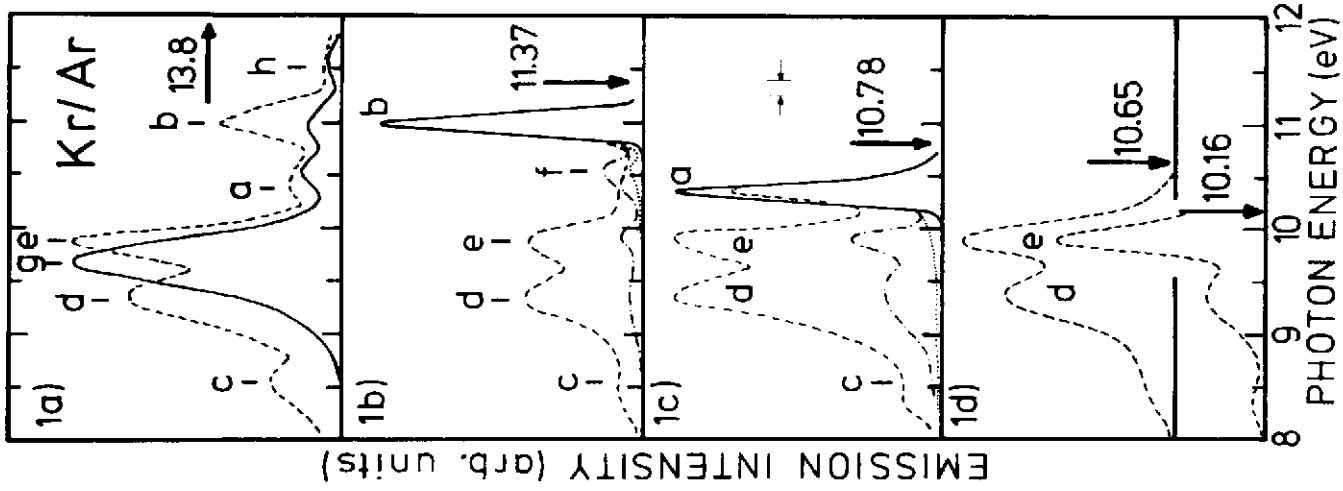

Table 4: Emission bands (E), lowest excitation maximum (absorption) (A) of Xe in Ar matrix and in the free atom (G). The emission bands are named as in Fig. 4. The assignment of earlier investigations is included. Energies in eV.

band	E	A	G	A-E	E-G	emission band E for excitation by α-particles[a]	electrons[b]	X-rays[c]	photons d)	photons e)	photons f)
d	8.32 site	8.57					8.28 $^3P_2$	8.28 $^3P_2$	8.32	8.27	8.36
							8.38 $^3P_1$	8.36 $^2P_1$			
c	8.42 site	9.02				8.38 $^3P_1$	8.40,8.46			8.44 $^3P_1$	8.50
							8.52,8.56			$^3P_2$	
							8.63:sites				
b	8.83 $^3P_1$	9.22 n=1	8.44	0.39	0,39	8.67 $^3P_1$s				8.70	
										9.40 $^1P_1$	
										9.61	
a	9.7 $^1P_1$n=2	9.95 n=2	9.57	0.25	0.23			9.88 $^1P_1$		9.80	9.90 $^1P_1$

For ref. a, b, c see table 1

d) T. Nanba, N. Nagasawa and M. Ueta, J. Phys. Sc. Jap. 37, 1031 (1974)

e) H. Möller, diploma work, Hamburg (1976)

f) Ch. Ackermann, thesis, Hamburg (1976)

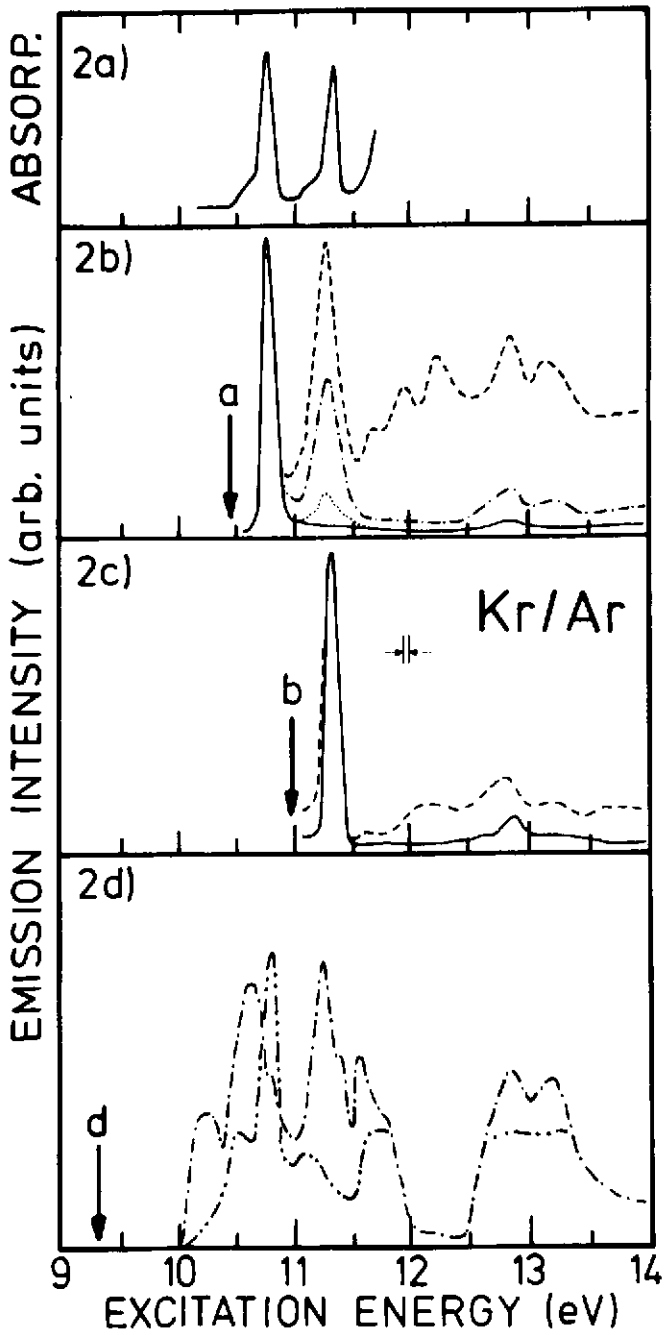
2a)
2b)
2c)
2d)
a
b
d
Kr/Ar
ABSORP.
EMISSION INTENSITY (arb. units)
9
10
11
12
13
14
EXCITATION ENERGY (eV)

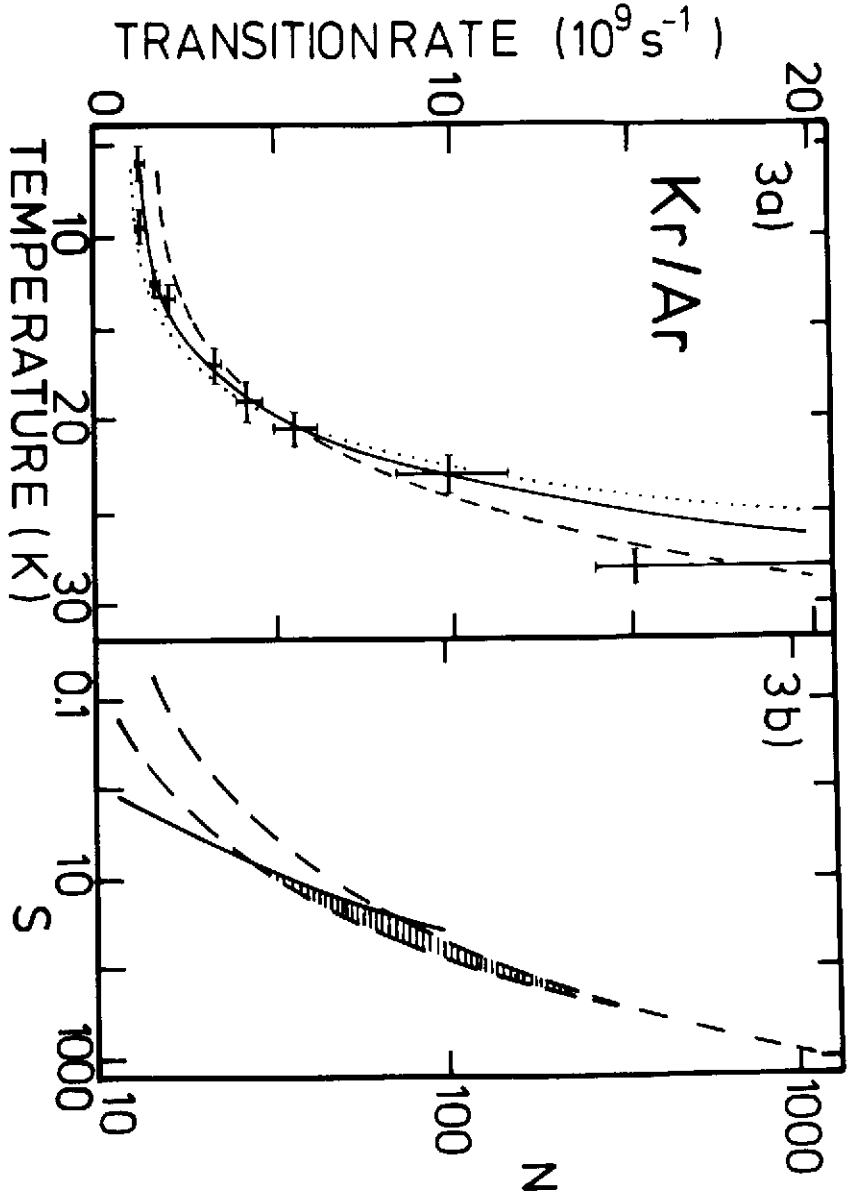
TRANSITION RATE ($10^9 s^{-1}$)
0
10
20
3a)
Kr/Ar
TEMPERATURE (K)
10
20
30
3b)
S
0.1
10
100
1000
10
100
1000
N

Fig. 4

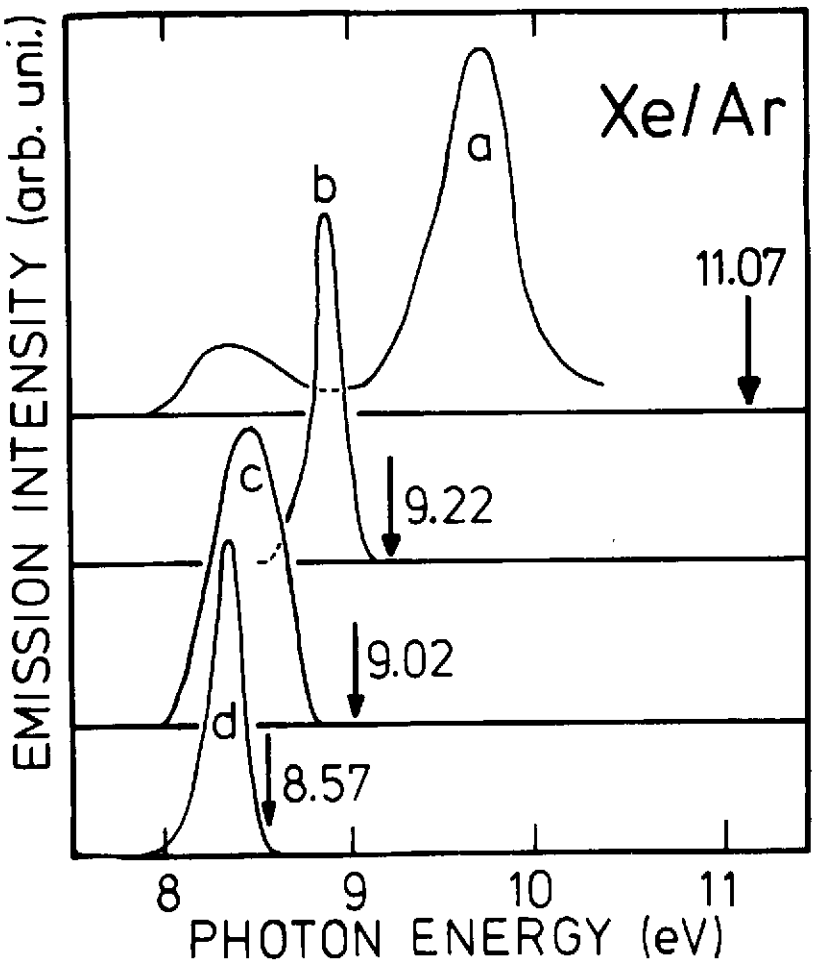
Xe/Ar
a
b
c
d
11.07
9.22
9.02
8.57
EMISSION INTENSITY (arb. uni.)
8
9
10
11
PHOTON ENERGY (eV)

Fig. 5

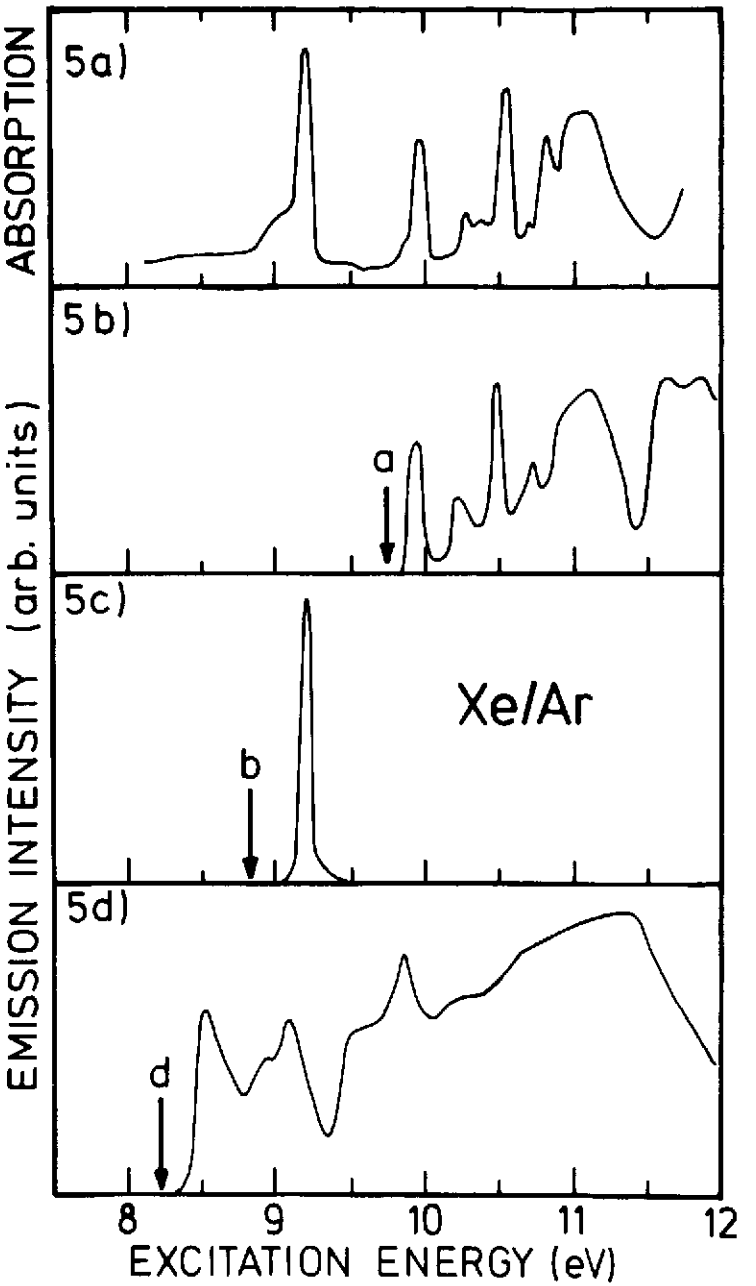
5a)
5b)
5c)
5d)
Xe/Ar
a
b
d
ABSORPTION
EMISSION INTENSITY (arb. units)
8
9
10
11
12
EXCITATION ENERGY (eV)